Available online at www.sciencedirect.com
SCIENCE DIRECT®
PERGAMON
Polyhedron 22 (2003) 867–873
POLYHEDRON
www.elsevier.com/locate/poly

Syntheses, structures and properties of *trans*-dichlororuthenium(II) complexes with N_4-donor Schiff bases

Satyanarayan Pal, Samudranil Pal *

School of Chemistry, University of Hyderabad, Hyderabad 500 046, India

Received 28 October 2002; accepted 9 December 2002

Abstract

The reactions of hydrated $RuCl_3$ and tetradentate Schiff bases (L = paen, papn and pabn) derived from 2-pyridine-carboxaldehyde and linear diamines such as 1,2-diaminoethane, 1,3-diaminopropane and 1,4-diaminobutane in boiling methanol afford complexes of general formula *trans*-[$RuLCl_2$]. The complexes were characterised by analytical, spectroscopic and electrochemical data. All the complexes are diamagnetic and electrically non-conducting. Thus in each complex the metal ion is in +2 oxidation state. The molecular structures of *trans*-[Ru(papn)Cl_2] and *trans*-[Ru(pabn)Cl_2] in the solid state have been determined by X-ray crystallography. In each molecule, the ruthenium(II) centre is in distorted octahedral N_4Cl_2 coordination sphere. The neutral ligand coordinates via two pyridine-N and two imine-N atoms forming a N_4 square-plane around the metal ion. The chloride ions satisfy the remaining two *trans* sites. The proton NMR spectra of all the complexes in $CDCl_3$ solutions are consistent with the *trans* arrangement of the chloride ions. Electronic spectra of the complexes in dichloromethane solutions display intense metal-to-ligand charge transfer bands in the range 595–656 nm. Cyclic voltammograms of the complexes in acetonitrile solutions display a reversible oxidation response in the potential range 0.26–0.40 V (vs. saturated calomel reference electrode) due to Ru^{III}/Ru^{II} couple.

Keywords: Ruthenium(II); Diimine ligands; Tetradentate; Syntheses; Structures

1. Introduction

Ruthenium(II) complexes with α,α′-diimine ligands, despite a vast literature, continue to be of current interest for their redox, photophysical and photochemical properties [1–11]. Majority of the complexes is with the polypyridine ligands such as 2,2′-bipyridine and 1,10-phenanthroline. This is mainly due to the presence of low-lying vacant π* orbitals in these ligands and hence the possibility of accessing low-energy metal-to-ligand (Ru(dπ) → L(π*)) charge transfer excited state that decides the physical properties of the complex. Such ruthenium complexes have important applications in artificial photosynthesis, photomolecular devices and elucidation of structural and electron transfer properties of proteins and DNA [12–16]. For this reason, there is a continuous pursuit for new ruthenium(II) complexes with derivatives of polypyridine ligands or with ligands containing the α,α′-diimine fragment [17–27]. Like 2,2′-bipyridine and 1,10-phenanthroline, Schiff bases derived from 2-pyridine-carboxaldehyde provide the π-acidic

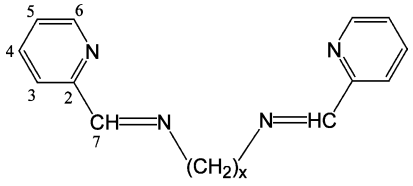

paen (x = 2)
papn (x = 3)
pabn (x = 4)

α,α′-diimine fragment for metal coordination. However, very few ruthenium(II) complexes with this type of Schiff bases are reported [25–27]. In the present work, we have studied the ruthenium(II) chemistry with a neutral tetradentate Schiff base ligand system (L = paen,

* Corresponding author. Tel.: +91-40-2301-0500; fax: +91-40-2301-2460.
E-mail address: spsc@uohyd.ernet.in (S. Pal).

0277-5387/03/$ - see front matter © 2003 Elsevier Science Ltd. All rights reserved.
doi:10.1016/S0277-5387(03)00008-1

papn and pabn) prepared from 2-pyridine-carboxaldehyde and diamines. Herein, we describe the synthesis and physical properties of three new ruthenium(II) complexes having the general formula *trans*-[RuLCl$_2$]. Solid state molecular structures of the complexes with papn and pabn determined by X-ray crystallography have been reported.

2. Experimental

2.1. Materials

The Schiff bases paen, papn and pabn were prepared by condensation of 2 mole equiv. of 2-pyridine-carboxaldehyde and 1 mole equiv. of the appropriate diamine ($H_2N(CH_2)_xNH_2$) in methanolic medium [28]. All other chemicals and solvents were of analytical grade available commercially and were used as received.

2.2. Physical measurements

Elemental (C, H, N) analysis data were obtained with a Perkin-Elmer Model 240C elemental analyser. Infrared spectra were collected by using KBr pellets on a JASCO-5300 FT-IR spectrophotometer. Room temperature solid state magnetic susceptibilities were measured by using a Sherwood Scientific magnetic susceptibility balance. Solution electrical conductivities were measured with a Digisun DI-909 conductivity meter. A Shimadzu 3101-PC UV–Vis–NIR spectrophotometer was used to record the electronic spectra. Proton NMR spectra of the complexes in $CDCl_3$ solutions were recorded on a Bruker 200 MHz spectrometer using $Si(CH_3)_4$ as an internal standard. A CH-Instruments model 620A electrochemical analyzer was used for cyclic voltammetric experiments with acetonitrile solutions of the complexes containing [(n-C_4H_9)$_4$N]ClO_4 (TBAP) as supporting electrolyte. The three electrode measurements were carried out at 298 K under a dinitrogen atmosphere with a platinum disk working electrode, a platinum wire auxiliary electrode and a saturated calomel reference electrode (SCE). Under identical condition the Fc^+/Fc couple is observed at $E_{\frac{1}{2}} = 0.41$ V.

2.3. Synthesis of trans-[Ru(paen)Cl$_2$] (1)

A methanol solution (15 ml) of $RuCl_3 \cdot 3H_2O$ (155 mg, 0.59 mmol) was refluxed for 6 h until the colour of the solution became green. To this green solution 190 mg (0.80 mmol) of paen in methanol (25 ml) was added and the mixture was refluxed for another 1 h. The purple reaction mixture was then evaporated to 1/5th of the original volume and $\sim$10 g of neutral aluminium oxide was added. This mixture was then dried in vacuum and transferred to a neutral aluminium oxide column packed using dichloromethane. The first moving blue band was eluted with dichloromethane–acetone (10:1) mixture. The blue solution of the complex collected was evaporated to dryness. The solid thus obtained was recrystallised from dichloromethane–hexane (1:1) mixture. Yield obtained was 62 mg (25%). *Anal.* Calc. for $C_{14}H_{14}N_4Cl_2Ru$: C, 40.99; H, 3.44; N, 13.66. Found: C, 40.64; H, 3.26; N, 13.52. Selected IR bands (cm^{-1}): 1593(s), 1561(m), 1528(s), 1454(s), 1422(s), 1325(m), 1242(w), 1204(m), 1146(w), 1103(w), 1061(m), 1003(m), 903(w), 818(w), 768(s), 644(w), 530(m), 517(s), 474(s).

2.4. Synthesis of trans-[Ru(papn)Cl$_2$] (2)

This complex was synthesised by using the same procedure and in 15% yield as described above by reacting $RuCl_3 \cdot 3H_2O$ and papn in methanol. *Anal.* Calc. for $C_{15}H_{16}N_4Cl_2Ru$: C, 42.46; H, 3.80; N, 13.20. Found: C, 42.31; H, 3.53; N, 13.10. Selected IR bands (cm^{-1}): 1597(s), 1568(m), 1537(s), 1458(s), 1429(s), 1296(w), 1221(m), 1146(m), 999(s), 909(m), 764(s), 640(m), 573(m), 523(s), 469(s).

2.5. Synthesis of trans-[Ru(pabn)Cl$_2$] (3)

This complex was also synthesised in methanolic medium by following the identical procedure used for the other two complexes in 10% yield from $RuCl_3 \cdot 3H_2O$ and pabn. *Anal.* Calc. for $C_{16}H_{18}N_4Cl_2Ru$: C, 43.84; H, 4.14; N, 12.78. Found: C, 43.61; H, 3.92; N, 12.55. Selected IR bands (cm^{-1}): 1597(s), 1570(m), 1537(s), 1456(s), 1427(s), 1356(w), 1333(w), 1289(m), 1229(s), 1144(s), 1037(w), 1011(m), 903(s), 822(w), 758(s), 638(m), 525(s), 492(s), 444(m).

2.6. X-ray crystallography

Single crystals of both *trans*-[Ru(papn)Cl$_2$] and *trans*-[Ru(pabn)Cl$_2$] were grown by slow evaporation of dichloromethane–hexane (1:1) solutions of the complexes. Data were collected on an Enraf-Nonius Mach-3 single crystal diffractometer using graphite monochromated Mo Kα radiation ($\lambda = 0.71073$ Å) by ω-scan method at 298 K. In each case, unit cell parameters were determined by least-squares fit of 25 reflections having 2θ values in the range 7°–22°. Intensities of 3 check reflections were measured after every 1.5 h during the data collection to monitor the crystal stability. In both cases, there is no significant change in the intensities of the check reflections. Empirical absorption correction was applied to each of the two datasets based on the ψ-scans [29] of 5 reflections in each case. The structures were solved by direct methods and refined on F^2 by full-matrix least-squares procedures. The methylene carbon

atoms in *trans*-[Ru(pabn)Cl_2] are disordered and each is located at two sites. They were refined with half occupancy and geometrical restraints. For *trans*-[Ru(papn)Cl_2], all non-hydrogen atoms and for *trans*-[Ru(pabn)Cl_2] non-hydrogen atoms having unit occupancy were refined using anisotropic thermal parameters. Hydrogen atoms were included in the structure factor calculation at idealised positions by using riding model, but not refined. The programs of WINGX [30] were used for data reduction and absorption correction. Structure solution and refinement were performed with the SHELX-97 programs [31]. The ORTEX6a package was used for molecular graphics [32]. Selected crystal and refinement data are listed in Table 1.

3. Results and discussion

3.1. Synthesis and some properties

Three Schiff bases (L) differing with regard to the spacer between the two picolinylaldimine fragments were obtained by the condensation of the 2-pyridinecarboxaldehyde and the appropriate diamine in 2:1 mole ratio in methanol. The reactions of hydrated $RuCl_3$ and L in boiling methanol affords a purple solution. Blue complexes were isolated from this reaction mixture by chromatographic work-up on a neutral alumina column. Elemental analysis data are consistent with the general formula $RuLCl_2$. The complexes are more soluble in less polar solvents such as $CHCl_3$ and CH_2Cl_2. In CH_3CN solutions, the complexes are electrically non-conducting. Thus the chloride ions are coordinated to the metal ion. The diamagnetic nature of all the three complexes is consistent with the +2 oxidation state and low-spin character of the metal ions in these complexes.

Table 1
Crystallographic data

Compound	*trans*-[Ru(papn)Cl_2]	*trans*-[Ru(pabn)Cl_2]
Chemical formula	$RuC_{15}H_{16}N_4Cl_2$	$RuC_{16}H_{18}N_4Cl_2$
Crystal system	monoclinic	monoclinic
Space group	$P2_1/m$	$C2/c$
a (Å)	6.9762(12)	13.665(3)
b (Å)	12.8372(19)	9.9511(13)
c (Å)	9.4254(14)	12.6283(17)
β (°)	100.45(2)	105.70(2)
V (Å^3)	830.1(2)	1653.1(4)
Z	2	4
Reflections measured	1998	2069
Reflections unique	1976	1893
Reflections $I > 2\sigma(I)$	1638	1031
Parameters	106	104
R_1 [a], wR_2 [b] ($I > 2\sigma(I)$)	0.0541, 0.2029	0.0748, 0.1430

[a] $R_1 = \Sigma||F_o|-|F_c||/\Sigma|F_o|$.

[b] $wR_2 = \{\Sigma[(F_o^2-F_c^2)^2]/\Sigma[w(F_o^2)^2]\}^{\frac{1}{2}}$; $w = 1/[\sigma^2(F_o^2)+(aP)^2+bP]$, where $a = 0.1293$ and 0.0637 and $b = 0.6890$ and 9.7599 for [Ru(papn)Cl_2] and [Ru(pabn)Cl_2], respectively.

3.2. Description of structures

The molecular structures of *trans*-[Ru(papn)Cl_2] (**2**) and *trans*-[Ru(pabn)Cl_2] (**3**) are shown in Figs. 1 and 2, respectively. Selected bond parameters associated with the metal ions are listed in Tables 2 and 3. In each structure, the asymmetric unit contains half of a complex molecule. In the case of **2**, two halves of the molecule are related by a crystallographically imposed mirror plane passing through the metal atom, the middle carbon atom (C8) of the trimethylene fragment and the two chlorine atoms (Fig. 1). On the other hand, two halves of a molecule of **3** are related by a twofold axis perpendicular to the Cl–Ru–Cl′ axis and passing through the metal atom and bisecting the tetramethylene fragment (Fig. 2). Two CH_2 groups in the asymmetric unit of **3** are disordered and located at four sites. For clarity, only one orientation of the four methylene groups are shown in Fig. 2. In each complex, the tetradentate ligand binds the metal ion through two pyridine-N and two imine-N atoms and forms a N_4 square-plane around the metal ion. The chlorine atoms occupy the remaining two mutually *trans* positions. The Cl–Ru–Cl angles are very close to the ideal value of 180° in both molecules (Tables 2 and 3). The chelate bite angles (77.4(2)° and 77.4(3)°) in the five-membered rings formed by the picolinylaldimine fragments are unexceptional [27] and identical in both complexes. The imine-N atoms form a six-membered and a seven-membered chelate ring in **2** and **3**, respectively. As expected, the chelate bite angle (97.1(3)°) in the six-membered ring is smaller than that (100.2(5)°) in the seven-membered ring. In the six-membered ring of **2**, the Ru, N2, C7, C7′ and N2′ atoms constitute a satisfactory plane with a mean deviation of 0.011 Å. However, C8 atom is displaced by 0.72(1) Å from this plane. Thus the six-membered chelate ring is folded along the C7, C7′ line and the fold angle is 62.7(6)°. The conformation of the seven-membered chelate ring in **3** is not clear due to disorder in the positions of the four carbon atoms of the

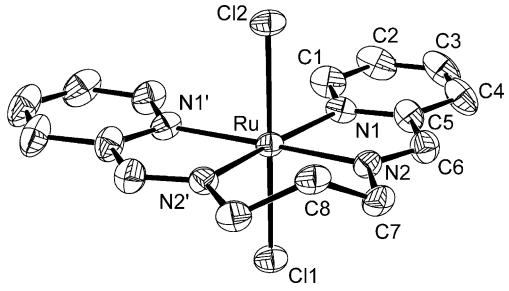

Fig. 1. Molecular structure of *trans*-[Ru(papn)Cl_2] with the atom-labelling scheme. All atoms are represented by their 30% probability thermal ellipsoids. Hydrogen atoms are omitted for clarity.

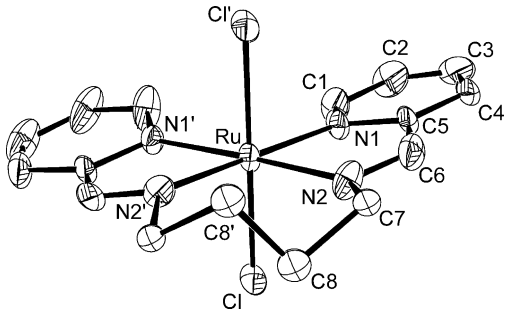

Fig. 2. Molecular structure of *trans*-[Ru(pabn)Cl_2] showing 30% probability thermal ellipsoids and the atom-labelling scheme. For clarity hydrogen atoms are omitted and one-set of the disordered methylene groups is shown.

Table 2
Selected bond lengths (Å) and angles (°) for *trans*-[Ru(papn)Cl_2] (**2**)

Ru–N(1)	2.099(5)	Ru–N(2)	1.979(5)
Ru–N(1′)	2.099(5)	Ru–N(2′)	1.979(5)
Ru–Cl(1)	2.396(2)	Ru–Cl(2)	2.394(2)
N(1)–Ru–N(2)	77.4(2)	N(1)–Ru–N(1′)	108.0(3)
N(1)–Ru–N(2′)	174.39(18)	N(1)–Ru–Cl(1)	91.82(14)
N(1)–Ru–Cl(2)	87.70(14)	N(2)–Ru–N(1′)	174.39(18)
N(2)–Ru–N(2′)	97.1(3)	N(2)–Ru–Cl(1)	89.51(14)
N(2)–Ru–Cl(2)	91.03(14)	N(1′)–Ru–N(2′)	77.4(2)
N(1′)–Ru–Cl(1)	91.82(14)	N(1′)–Ru–Cl(2)	87.70(14)
N(2′)–Ru–Cl(1)	89.51(14)	N(2′)–Ru–Cl(2)	91.03(14)
Cl(2)–Ru–Cl(1)	179.19(7)		

Symmetry transformation used to generate equivalent atoms: x, $-y+\frac{1}{2}$, z.

Table 3
Selected bond lengths (Å) and angles (°) for *trans*-[Ru(pabn)Cl_2] (**3**)

Ru–N(1)	2.085(7)	Ru–N(2)	2.030(7)
Ru–N(1′)	2.085(7)	Ru–N(2′)	2.030(7)
Ru–Cl(1)	2.411(2)	Ru–Cl(1′)	2.411(2)
N(1)–Ru–N(2)	77.4(3)	N(1)–Ru–N(1′)	105.1(5)
N(1)–Ru–N(2′)	177.2(4)	N(1)–Ru–Cl	91.2(2)
N(1)–Ru–Cl′	87.6(2)	N(2)–Ru–N(1′)	177.2(4)
N(2)–Ru–N(2′)	100.2(5)	N(2)–Ru–Cl	91.2(3)
N(2)–Ru–Cl′	90.1(3)	N(1′)–Ru–N(2′)	77.4(3)
N(1′)–Ru–Cl	87.6(2)	N(1′)–Ru–Cl′	91.2(2)
N(2′)–Ru–Cl	90.1(3)	N(2′)–Ru–Cl′	91.2(3)
Cl–Ru–Cl′	178.03(17)		

Symmetry transformation used to generate equivalent atoms: $-x$, y, $-z+3/2$.

tetramethylene fragment. The Ru(II)–N(pyridine) bond lengths are similar in both complexes and within the range reported for ruthenium(II) complexes having the same coordinating atom [27,33]. The Ru(II)–N(imine) bond length (1.979(5) Å) in **2** is comparable with those reported earlier [24,27]. However, the same bond length (2.030(7) Å) is significantly longer in **3**. This is likely to be the consequence of the larger chelate ring size formed by the imine-N atoms of pabn compared to that formed by the imine-N atoms of papn. The Ru(II)–Cl distances are in the range 2.394(2)–2.411(2) Å and similar to the Ru–Cl bond lengths found in complexes of *trans*-dichlororuthenium(II) [33,34].

3.3. Spectral characteristics

Infrared spectra of the complexes display a strong peak at $\sim$1595 cm^{-1}. In free L, the $\nu_{C=N}$ of the azomethine fragment is observed at $\sim$1645 cm^{-1}. This frequency is expected to be lower in the complexes. Thus the origin of the peak at $\sim$1595 cm^{-1} might involve the –HC=N– group of the metal coordinated Schiff bases [25–27]. Three medium to strong peaks observed in the range 1570–1454 cm^{-1} are likely to be associated with the pyridine rings of the ligands [35].

The ^{1}H NMR spectra of the complexes have been recorded in $CDCl_3$ solutions to probe the solution structures. The proton numbering scheme is shown in the chemical diagram of the Schiff base system. The spectral data are listed in Table 4. For each of the three complexes, only one set of protons corresponding to the picolinylaldimine moieties of the ligand appear in the range 7.5–9.5 δ. A multiplet centred at $\sim$7.84 δ corresponding to two protons and another multiplet in the range 7.56–7.68 δ corresponding to a single proton are observed. The former is assigned to the 3-H and 4-H and the latter is assigned to the 5-H. The 6-H proton appears as a doublet within 9.20–9.43 δ. The azomethine proton (7-H) is observed as a singlet in the rang 8.95–9.25 δ. An interesting trend in the position of this signal is that as the chelate ring size formed by the two imine-N atoms of the Schiff base system increases the signal displays a high-field shift. In the spectrum of **1**, a singlet corresponding to two protons is observed at 4.82 δ. This signal is assigned to the methylene group protons. Appearance of the protons of a solitary methylene group as a singlet suggests that not only two picolinylaldimine fragments but also two methylene groups of the complexed paen in **1** are magnetically equivalent, at least on an NMR time-scale. This observation is consistent with the chlorides being mutually *trans* in **1**. In the spectrum of **2**, a triplet and a quintet are observed at 4.55 and 2.64 δ, respectively. The intensity of the triplet is twice that of the quintet. The former is assigned to the protons of the terminal methylene groups and the latter is assigned to the middle methylene group protons of the trimethylene fragment of the ligand papn. Appearance of a triplet for the terminal methylene group protons and a quintet for the central methylene group protons clearly indicates that two halves of the papn in **2** are magnetically equivalent. Thus in solution, **2** has the same *trans* structure with respect to the two chlorides as observed in the solid state. Two multiplets of equal intensity are observed at 4.72 and 2.46 δ in the spectrum of **3**. The multiplet at

Table 4
Electronic absorption[a] and ^{1}H NMR[b] spectral data for *trans*-[RuLCl$_2$]

Complex	λ_{max} (nm) ($10^3 \times \varepsilon$ (M^{-1} cm^{-1}))	δ (ppm) (J (Hz)) [c]					
		H(3)/H(4)	H(5)	H(7)	H(6)	H(8)	H(9)
1	900 (0.14), 804 (0.18), 595 (16.7), 375 (4.1), 352 [d] (3.6), 274 (14.6)	7.83m	7.68m	9.25s	9.20d (5)	4.82s	–
2	930 (0.16), 808 (0.21), 650 [d] (11.6), 612 (13.5), 402 (4.1), 363 [d] (3.4), 282 (12.9)	7.85m	7.61m	9.14s	9.43d (6)	4.55t (4)	2.64q (4)
3	929 (0.20), 806 (0.25), 656 (10.6), 610 (11.6), 409 (4.0), 368 [d] (3.3), 281 (14.5)	7.84m	7.56m	8.95s	9.42d (5)	4.72m	2.46m

[a] In dichloromethane solution.
[b] In $CDCl_3$ solution.
[c] Symbols: s, singlet; d, doublet; t, triplet; q, quintet; m, multiplet.
[d] Shoulder.

the lower field is assigned to the methylene group protons attached to the azomethine nitrogen and the multiplet at higher field is assigned to the following methylene group protons. Observation of only two signals for the methylene groups of the tetramethylene fragment of pabn in **3** is consistent with the *trans*-dichloro structure in solution similar to that determined in the solid state.

The dichloromethane solutions of the complexes are blue in colour. The electronic absorption spectral data collected using these blue solutions are listed in Table 4. The complexes display several bands in the range 930–274 nm (Fig. 3). The spectral profiles below 450 nm are very similar. In this region, a strong peak in the range 409–375 nm followed by a shoulder within 368–352 nm and another strong peak in the range 282–274 nm are observed (Table 4). These absorptions are likely to be due to intraligand transitions. Above 500 nm all the complexes display strong absorptions ($\varepsilon \approx 10^4$ M^{-1} cm^{-1}) in the range 595–656 nm due to metal-to-ligand ($Ru(d\pi) \rightarrow L(\pi^*)$) charge transfer transitions (MLCT). An interesting trend in the MLCT band positions of these complexes are as follows. Complex **1** displays a single peak at 595 nm. On the other hand, for complex **2** the peak at 612 nm is preceded by a shoulder at 650 nm and for complex **3** two peaks are observed at 610 and 656 nm. Broad or multiple MLCT bands in this type of complexes are not unusual due to the availability of several acceptor levels of different but similar energies [25–27,34,36]. It may be noted that the complexes **1**, **2**, and **3** differ only in the central chelate ring size formed by the two imine-N atoms of the Schiff bases. The chelate ring is five-membered in **1**, six-membered in **2** and seven-membered in **3**. All the three complexes display two weak absorptions in the wavelength range 930–804 nm (Table 4). These absorptions are most likely due to singlet–triplet transitions made allowed by strong spin-orbit coupling in ruthenium [25,34,36–38].

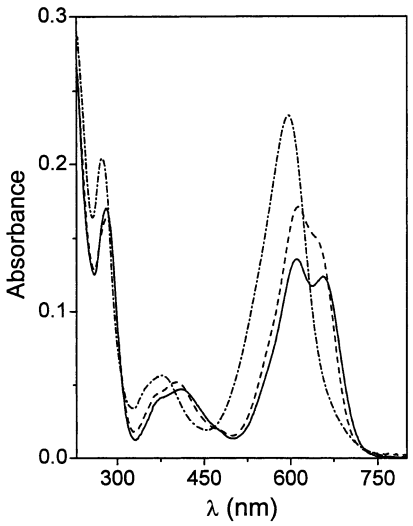

Fig. 3. Electronic absorption spectra of *trans*-[Ru(paen)Cl$_2$] (0.14×10^{-4} M) (-·-·-·-), *trans*-[Ru(papn)Cl$_2$] (0.13×10^{-4} M) (- - - -) and *trans*-[Ru(pabn)Cl$_2$] (0.12×10^{-4} M) (—) in dichloromethane solutions.

3.4. Redox properties

Electron transfer properties of all the three complexes in acetonitrile solutions (0.1 M TBAP) have been investigated by cyclic voltammetry using a platinum disk working electrode and a SCE. Each complex displays a metal centred one-electron oxidation response on the anodic side of SCE (Table 5). A representative voltammogram is shown in Fig. 4. The one-electron stoichiometry of this electron transfer process is established by comparing the current height with known one electron redox processes under identical conditions

Table 5
Cyclic voltammetric[a,b] data for *trans*-[RuLCl$_2$]

Complex	$E_{1/2}$ (V) (ΔE_p (mV))	E_{pc} (V)
1	0.40 (70)	−1.34
2	0.28 (60)	−1.37, −1.47
3	0.26 (70)	−1.42, −1.53

[a] In acetonitrile solution at 298 K at a scan rate of 50 mV s^{-1}.
[b] $E_{\frac{1}{2}} = (E_{pa} + E_{pc})/2$, where E_{pa} and E_{pc} are anodic and cathodic peak potentials, respectively; $\Delta E_p = E_{pa} - E_{pc}$.

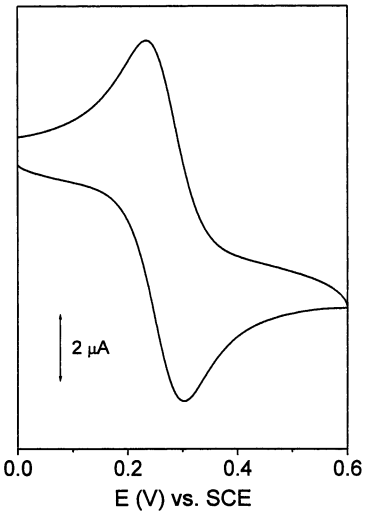

Fig. 4. Cyclic voltammogram of *trans*-[Ru(pabn)Cl_2] in acetonitrile solution (0.1 M TBAP) at a scan rate of 50 mV s^{-1}.

[27,39]. The reversible character of the Ru(II) → Ru(III) oxidation is evident from the peak-to-peak separation of 60–70 mV and almost equal anodic (i_{pa}) and cathodic peak currents (i_{pc}).

All the complexes display irreversible ligand based one-electron reductions on the cathodic side of SCE (Table 5). Complex **1** shows only one reduction at −1.34 V. On the other hand, both **2** and **3** display two reductions with a separation of 100–110 mV. Interestingly, **2** and **3** display two closely spaced MLCT bands in the electronic absorption spectra, whereas **1** displays only one MLCT band (Table 4). The MLCT transitions involve excitation of metal dπ electrons to the π* orbitals of ligand which are also involved in electrochemical reductions. It has been noted before that for this type of Ru(II) complexes, the MLCT band positions and the electrode potentials associated with the metal ion oxidation and ligand reduction are correlated and reflect the relative energies of the metal dπ and ligand π* levels [4,26,27,34,36]. As mentioned before the difference in the molecular structures of **1**, **2** and **3** is the central chelate ring size formed by the imine-N atoms of the ligands. Possibly for **2** and **3** with six-membered and seven-membered central chelate ring, respectively there is a small but detectable energy difference between two lowest energy acceptor levels but for **1** having the smallest five-membered ring size the concerned acceptor levels are essentially of same energy. The observations of two MLCT bands and two ligand based reductions for **2** and **3** and single MLCT band and single ligand based reduction are consistent with such a situation.

The Ru(II) → Ru(III) oxidation potentials for **2** and **3** are within 20 mV (Table 5). However, the potential for **1** is 130 mV higher than the average of the potentials of **2** and **3**. On the other hand, the first ligand reduction potentials of these complexes are in a relatively narrow range of −1.34 to −1.42 V. A possible rationale for the above trends in the potential values is as follows. Most likely ligand π* levels are of comparable energy in all the three complexes but the metal dπ level is relatively more stabilised in **1** than the dπ levels in **2** and **3**. As a result Ru(II) → Ru(III) oxidation in **1** becomes more difficult and is observed at higher potential. The trend in the MLCT band positions (Table 4) of **1**, **2** and **3** also supports this conjecture. Such a situation may also be another consequence of the difference in the central chelate ring size in these complexes.

4. Conclusions

The present work describes the synthesis and physical properties of three new *trans*-dichlororuthenium(II) complexes with tetradentate Schiff bases prepared from 2-pyridine-carboxaldehyde and linear diamines. The solid state molecular structures of two complexes determined by X-ray crystallography confirm the *trans*-[$RuLCl_2$] formulation. Proton NMR spectra of all the complexes are consistent with the same *trans* arrangement of chlorides in solution. Complexes display intense MLCT transitions in the electronic spectra. Cyclic voltammetric studies reveal that the complexes are redox active. The influence of the chelate ring size formed by the imine-N atoms of the Schiff base on the MLCT band positions and the redox potentials are noted. These complexes appear to be useful starting materials for the synthesis of oxo/hydroxo coordinated mononuclear as well as polynuclear ruthenium species by the replacement of the chloride ligands under appropriate conditions. We are currently involved in exploring such possibilities.

5. Supplementary material

Crystallographic data have been deposited with the Cambridge Crystallographic Data Centre (deposition numbers CCDC No. 195234 and CCDC No. 195235). Copies of this information may be obtained from The Director, CCDC, 12 Union Road, Cambridge, CB2 1EZ, UK (fax: +44-1223-336033; e-mail: deposit@ccdc.cam.ac.uk or http://www.ccdc.cam.ac.uk).

Acknowledgements

Financial support by the Department of Science and Technology (DST), New Delhi (Grant No. SP/S1/F23/99) is gratefully acknowledged. Mr Satyanarayan Pal thanks the Council of Scientific and Industrial Research, New Delhi for a research fellowship. X-ray crystallographic studies were performed at the DST funded

National Single Crystal Diffractometer Facility, School of Chemistry, University of Hyderabad.

References

[1] E.A. Seddon, K.R. Seddon, The Chemistry of Ruthenium, Elsevier, New York, 1984.
[2] G. Wilkinson, R.D. Gillard, J.A. McCleverty, Comprehensive Coordination Chemistry, vol. 4, Pergamon, Oxford, 1987, p. 277.
[3] A. Juris, V. Balzani, F. Barigelletti, S. Campagna, P. Belser, A. von Zelewsky, Coord. Chem. Rev. 84 (1988) 85.
[4] B.K. Ghosh, A. Chakravorty, Coord. Chem. Rev. 95 (1989) 239.
[5] A.B.P. Lever, H. Masui, R.A. Metcalfe, D.J. Stufkens, E.S. Dodsworth, P.R. Auburn, Coord. Chem. Rev. 125 (1993) 317.
[6] J.-P. Sauvage, J.-P. Collin, J.-C. Chambron, S. Guillerez, C. Coudret, V. Balzani, F. Barigelletti, L. De Cola, L. Flamigni, Chem. Rev. 94 (1994) 993.
[7] V. Balzani, A. Juris, M. Venturi, S. Campagna, S. Serroni, Chem. Rev. 96 (1996) 759.
[8] S.-M. Lee, W.-T. Wong, Coord. Chem. Rev. 164 (1997) 415.
[9] S.I. Gorelsky, E.S. Dodsworth, A.B.P. Lever, A.A. Vlcek, Coord. Chem. Rev. 174 (1998) 469.
[10] L. De Cola, P. Belser, Coord. Chem. Rev. 177 (1998) 301.
[11] K. Szaciowski, W. Macyk, G. Stochel, Z. Stasicka, S. Sostero, O. Traverso, Coord. Chem. Rev. 208 (2000) 277.
[12] L. Sun, L. Hammarström, B. Åkermark, S. Styring, Chem Soc. Rev. 30 (2001) 36.
[13] P.D. Beer, Acc. Chem. Res. 31 (1998) 71.
[14] N. Sardesai, S.C. Lin, K. Zimmermann, J.K. Barton, Bioconjugate Chem. 6 (1995) 302.
[15] H.B. Gray, J.R. Winkler, Annu. Rev. Biochem. 65 (1996) 537.
[16] P. Lincoln, E. Tuite, B. Nordén, J. Am. Chem. Soc. 119 (1997) 1454.
[17] M. Ziegler, V. Monney, H. Stoeckli-Evans, A. von Zelewsky, I. Sasaki, G. Dupic, J.C. Daran, G.G.A. Balavoine, J. Chem. Soc., Dalton Trans. (1999) 667.
[18] J.E. Collins, J.J.S. Lamba, J.C. Love, J.E. McAlvin, C. Ng, B.P. Peters, X. Wu, C.L. Fraser, Inorg. Chem. 38 (1999) 2020.
[19] B. Geisser, A. Ponce, R. Alsfasser, Inorg. Chem. 38 (1999) 2030.
[20] A. Juris, L. Prodi, A. Harriman, R. Ziessel, M. Hissler, A. Elghayoury, F. Wu, E.C. Riesgo, R.P. Thummel, Inorg. Chem. 39 (2000) 3590.
[21] X. Zhou, D.S. Tyson, F.N. Castellano, Angew. Chem., Int. Ed. 39 (2000) 4301.
[22] L.H. Uppadine, M.G.B. Drew, P.D. Beer, Chem. Commun. (2001) 291.
[23] H. Chao, G. Yang, G.Q. Xue, H. Li, H. Zang, I.D. Williams, L.N. Ji, X.M. Chen, X.Y. Li, J. Chem. Soc., Dalton Trans. (2001) 1326.
[24] A.K. Das, S.M. Peng, S. Bhattacharya, Polyhedron 20 (2001) 327.
[25] S. Choudhury, M. Kakoti, A.K. Deb, S. Goswami, Polyhedron 11 (1992) 3183.
[26] S. Choudhury, A.K. Deb, S. Goswami, J. Chem. Soc., Dalton Trans. (1994) 1305.
[27] S.N. Pal, S. Pal, J. Chem. Soc., Dalton Trans. (2002) 2102.
[28] B. Chiswell, Inorg. Chim. Acta 12 (1975) 195.
[29] A.C.T. North, D.C. Philips, F.S. Mathews, Acta Crystallogr., Sect. A 24 (1968) 351.
[30] L.J. Farrugia, J. Appl. Crystallogr. 32 (1999) 837.
[31] G.M. Sheldrick, SHELX-97, University of Göttingen, Göttingen, Germany, 1997.
[32] P. McArdle, J. Appl. Crystallogr. 28 (1995) 65.
[33] S.N. Pal, S. Pal, Acta Crystallogr., Sect. C 58 (2002) m273.
[34] T.K. Misra, D. Das, C. Sinha, P. Ghosh, C.K. Pal, Inorg. Chem. 37 (1998) 1672.
[35] W. Kemp, Organic Spectroscopy, Macmillan, Hampshire, 1987, p. 56.
[36] P. Byabartta, J. Dinda, P.K. Santra, C. Sinha, K. Panneerselvam, F.-L. Liap, T.-H. Lu, J. Chem. Soc., Dalton Trans. (2001) 2825.
[37] S. Decurtins, F. Felix, J. Ferguson, H.U. Güdel, A. Ludi, J. Am. Chem. Soc. 102 (1980) 4102.
[38] E.M. Kober, T.J. Meyer, Inorg. Chem. 21 (1982) 3967.
[39] S.N. Pal, S. Pal, Inorg. Chem. 40 (2001) 4807.